

# Microkinetic modeling applied to catalytic cracking of paraffins

Pedro Miguel Lopes Gomes

Instituto Superior Técnico, Av. Rovisco Pais, 1049-001 Lisbon, Portugal

**Abstract:** In order to optimize the efficiency of the FCC process for a certain target, a better understanding of its complex reaction network is required. The purpose of this work is to develop a microkinetic lumped model with a small parameter set, capable of making accurate and detailed predictions of the product distribution for the catalytic cracking of paraffins, independently of their size which could later be applied to real FCC feedstocks. To reduce the number of individual rate constants, these are organized by reaction families and calculated through empirical equations based on the nature of species involved and of the reaction involved, while the lumps are organized by number of carbon atoms and by chemical family. The model is fitted to experimental results using n-heptane and then tested for n-hexane and n-octane. The experimental data corresponds to catalytic cracking over an H-ZSM-5 catalyst. The model still requires further development, mainly in the prediction of the molar fraction of propane which is one of the main products for these feedstocks. This is clear in the simulations for n-heptane and n-octane. However, in the simulations for n-hexane, the model can make a good prediction of the molar fractions not only of propane, but also the rest of the product distribution. This may indicate that the problem should be related to the symmetry of the protolytic scission reaction.

## Introduction

The catalytic cracking mechanism of paraffins is a matter that has not been yet fully understood although there are some main theories that are generally accepted to explain it.

It is believed that catalytic cracking of paraffins occurs as a chain reaction according to the Whitmore carbenium ion theory [1]. Despite all the discussion about how catalytic cracking is initiated, consensus has been reached about the type of acid sites responsible for the initiation of catalytic cracking: Brønsted acid sites. Brønsted acid sites can ensure some stability to the

adsorbed carbenium ion [2] [3]. However, Lewis acid sites also have an important role during the propagation step [4].

Some authors suggested that the formation of the carbenium ions occurs due to the protonation of an olefin present in the feed by a Brønsted acid site [5] followed by a hydride abstraction from a gas phase paraffin to form a new carbenium ion [6]. Later, other authors suggested the formation of a penta-coordinated carbonium ion by direct protonation of paraffin [7].

The classic mechanism for the catalytic cracking is a bimolecular mechanism proposed by Greensfelder [6] and consists on gas phase paraffin carrying out a hydride

transfer with a carbenium ion that is already adsorbed which results in a new carbenium ion adsorbed and the desorption of the previous one. The new carbenium ion will then crack, by  $\beta$ -scission producing an olefin and a smaller carbenium ion and this carbenium ion will take part on hydride transfer reactions with some other gas phase paraffin to restart the cycle. A scheme to illustrate this reactional cycle is presented in Figure 1.

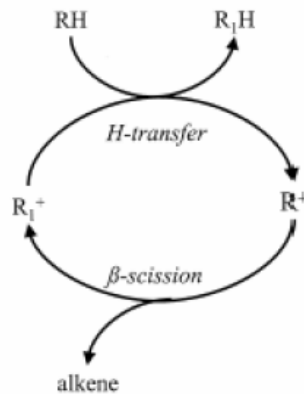


Figure 1 – Reactional cycle of the traditional bimolecular mechanism for catalytic cracking of paraffins [8].

Although this mechanism has been generally accepted, it has some limitations to its applicability: it requires pre-existing carbenium ions and cannot explain the appearance of dry gas in the product distribution.

An alternative mechanism for the initiation step of the catalytic cracking of paraffins as proposed by Haag and Dessau [7] is called protolytic scission. This is a monomolecular mechanism in which a strong Brønsted acid site protonates a paraffins, with higher tendency to happen on the most substituted carbon atom, forming a pentacoordinated carbonium ion. This is a very instable intermediate state and it soon drops a molecule of H<sub>2</sub> or a smaller paraffin to form carbenium ion also smaller than the

original paraffin. This alternative mechanism, when compared with the traditional one, has the advantages of not needing the pre-existence of carbenium ions and it can also explain the formation of molecular hydrogen, methane and ethane. A scheme to illustrate the protolytic scission is presented in Figure 2.

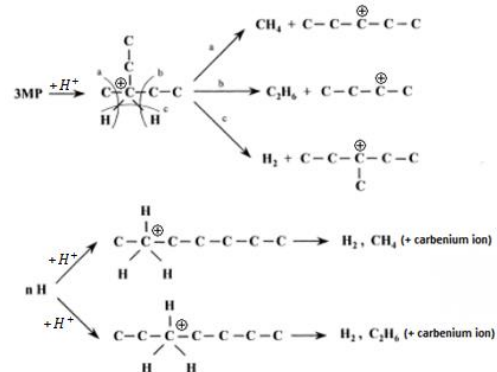


Figure 2 - Protolytic scission mechanism for linear and branched paraffins (adapted) [9].

The relative contribution of each of cracking mechanism depends on the nature of the feed, catalyst and operating conditions. Protolytic scission is favored by high temperatures, low partial pressure, low acid site densities and low conversions of reactant [7] while  $\beta$ -scission is favored by lower temperatures [10][11]. Smaller pores have increased shape selectivity and tend to favor protolytic scission because its transition state is smaller than the one from the bimolecular hydride transfer reaction prior to  $\beta$ -scission [9]. This can be observed when comparing ZSM5 with Y, the first one, which has smaller pores, favors protolytic scission [7]. Also, catalyst with high Si/Al ratios tend to favor protolytic scission because this reactions requires stronger Brønsted acid sites and their strength increases with Si/Al ratio, while  $\beta$ -scission is favored by high acid sites concentrations

and high adsorption capacity, which decrease with Si/Al ratio [12].

The propagation step for the catalytic cracking of paraffins can take several routes, independently of the origin of the initiation step to form the carbenium ion. One possible route is the carbenium ion undergoing  $\beta$ -scission and form a smaller olefin and a smaller carbenium ion than the original one. The carbenium ion can also undergo the traditional bimolecular mechanism by abstracting hydride ion from a paraffin. It can also undergo oligomerization with an olefin forming a larger carbenium ion. It can also isomerize and then take any of the previous routes [9].

The carbenium ion can also desorb from the acid site and form an olefin while regenerating the Brønsted acid site. This is considered a termination step for the chain reaction for the catalytic cracking of olefins.

Several microkinetic models have been developed related to catalytic cracking of hydrocarbons. There are 3 types of microkinetic models: mechanistic models, pathways-level models and lumped models [13].

Mechanistic models accounts a huge amount of molecules likewise the intermediary states which allows them to provide fundamental kinetic information and detailed molecular representation. However, the complexity of these models does not allow them to present a solution in a reasonable time [13].

On lumped models compounds with physical and/or chemical properties in common are grouped and the kinetic behavior is studied between these groups called lumps. This fact makes this type of

models the most used in catalytic cracking microkinetic modeling because they very useful when a large number of compounds is being considered. However, the application of this type of model to the FCC most of times ignores the complexity of its reaction network which limits its application to a specific feedstock [13].

Pathways models are a kind of compromise between the previous types of microkinetic models. They can make a detailed prediction of the product distribution, which most lumped models cannot, because every observable molecule is accounted in the model. At the same time, this type of microkinetic models can provide a solution in a reasonable time, which mechanistic models cannot, because they do not have in account all the intermediary species reducing drastically the number of chemical species accounted in the model [13].

## Methodology

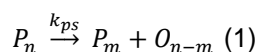
In this work it is purposed a 60-lump model to study the complex reaction network of catalytic cracking of paraffins. The aim of this model is to make accurate and detailed predictions of the product distribution while using a limited number of parameters. Also, the model predictions should be independent of feedstock composition and the amount of reactant. However, the data available to test this model is limited to a specific temperature (450 ° C) and catalyst (H-ZSM5).

In order to develop this model, several factors were taken into account:

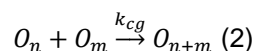
- The molecules have been lumped by the number of carbon atoms of each compound and by chemical family accounting linear paraffins, branched paraffins and olefins, up to 20 carbon atoms
- The only aromatics accounted for in the model have 6, 7 and 8 carbon atoms.
- The coke formed is accounted as an olefin with 21 carbon atoms which is not accounted for on the flow calculations since it remains adsorbed on the catalyst.
- Intermediary species, such as carbenium and carbonium ions, are not explicitly accounted for in this model and the reactions are considered to happen in a pseudo gaseous phase.
- The model accounts a total of 60 different species (20 n-paraffins, 20 i-paraffins, 20 olefins and 3 aromatics) and 1582 reactions between them.
- Reactions are lumped by families and their constant rates are estimated by empirical equations, one for each family of reactions and with a small set of parameters.
- The rate constants depend only on the size and the nature of the reactant molecules.

The reaction families considered in the model are:

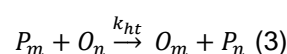
- Protolytic scission: a paraffin “cracks” into a smaller paraffin and an olefin with the remaining carbon atoms



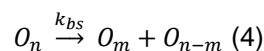
- Chain growth: an olefin reacting with other olefin thus forming a bigger one.



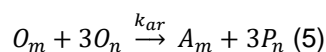
- Hydride transfer: abstraction of a hydride ion from a paraffin by an olefin forming an olefin with same number of carbon atoms of reacting paraffin and a paraffin with same number of carbon atoms of reacting olefin (the other hydrogen ion belongs to the catalyst acid site).



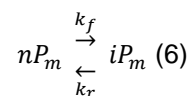
- $\beta$ -scission: the opposite of the chain growth reaction, a bigger “olefin cracks” into 2 smaller olefins.



- Aromatic formation: an olefin cyclizes and transfers 6 hydrogen atoms to 3 olefins forming an aromatic and 3 paraffins. The olefins that cyclizes has 6, 7 or 8 carbon atoms while the 3 olefins that form paraffins have the same carbon atoms.



- Isomerization: a linear paraffin rearranges into a branched paraffin.



- The branched paraffins will also react through protolytic scission and hydride transfer. The products will be linear paraffins and olefins.

$$iP_n \xrightarrow{k_{ps}} nP_m + O_{n-m} \quad (7)$$

$$iP_m + O_n \xrightarrow{k_{ht}} O_m + nP_n \quad (8)$$

## Mass Balance

The mass balance to the reactor is described by equation 9, where: the variation of the number of moles throughout the time for a certain compound, with  $i$  carbon atoms of the  $j$  type, depends on the difference between its entry and outlet flows, and its global reaction rate.

$$\frac{dN_{(i,j)}}{dt} = F_{(i,j)}^e - F_{(i,j)}^o + r_{(i,j)} \quad (9)$$

## Global Reaction Rates

The global reaction rates for each species is obtained by the sum of all the reaction rates where a certain compound is involved. Equations 10-14 describe the global reaction rates for each type of molecule, where  $j=1$  represents linear paraffins,  $j=2$  represents branched paraffins,  $j=3$  represents olefins and  $j=4$  represents aromatics. The indexes  $n$  and  $m$  are related to the indexes from equations 1-8.

- Linear paraffins:

$$r_{(i,1)} = \sum r_{ps(i=m)} - \sum r_{ps(i=n,1)} + \sum r_{ht(i=n)} - \sum r_{ht(i=m,1)} + 3 \sum r_{ar(i=n)} - \sum r_{iso(i=n)} \quad (10)$$

- Branched paraffins:

$$r_{(i,2)} = \sum r_{iso(i=n)} - \sum r_{ps(i=n,2)} - \sum r_{ht(i=m,2)} \quad (11)$$

- Olefins:

$$r_{(i,3)} = \sum r_{ps(i=n-m)} + \sum r_{ht(i=m)} - \sum r_{ht(i=n)} + \sum r_{cg(i=n+m)} - \sum r_{cg(i=n)} -$$

$$\sum r_{cg(i=m)} + \sum r_{bs(i=m)} + \sum r_{bst(i=n-m)} - \sum r_{bs(i=n)} - \sum r_{ar(i=m)} - 3 \sum r_{ar(i=n)} \quad (12)$$

- Aromatics:

$$r_{(i,4)} = \sum r_{ar(i=n)} \quad (13)$$

- Coke:

$$r_{(21,3)} = \sum r_{cg(n+m \geq 21)} \quad (14)$$

## Elementary Step Reaction Rates

The elementary step reaction rates were calculated through equations 15-20, where a generic  $k_{(n,m)}$  represents rate constant,  $w$  represents the mass of catalyst, and a generic  $P_{(i,j)}$  represents the partial pressure of certain specie. The indexes  $n$  and  $m$  are related to the indexes from equations 1-8.

- Protolytic scission:

$$r_{ps(n,m)} = k_{ps(n,m)} \times P_{(n,1 \text{ or } 2)} \times w \quad (15)$$

- Chain growth:

$$r_{cg(n,m)} = k_{cg(n,m)} \times P_{(n,3)} \times P_{(m,3)} \times w \quad (16)$$

- Hydride transfer:

$$r_{ht(n,m)} = k_{ht(n,m)} \times P_{(n,3)} \times P_{(m,1 \text{ or } 2)} \times w \quad (17)$$

- $\beta$ -scission:

$$r_{bs(n,m)} = k_{bs(n,m)} \times P_{(n,3)} \times w \quad (18)$$

- Aromatic formation:

$$r_{ar(n,m)} = k_{ar(n,m)} \times P_{(m,3)} \times P_{(n,3)}^3 \times w \quad (19)$$

- Isomerization:

$$r_{iso} = k_{iso(n)} \left( P_{(n,1)} - \frac{P_{(n,2)}}{K(n)} \right) \times w \quad (20)$$

The proceeding to calculate the constant rates likewise to calculate the isomerization elementary step reaction rates will be further explain in the results section.

## Constant Rates

Protolytic Scission: the rate constant was calculated using equation 20 adapted from Pinto [14], where  $k_{0ps}$  accounts for the intensity of the protolytic scission reaction;  $a_{ps}$  relates to the rate of reaction with the reacting paraffin;  $b_{ps}$  relates to the rate of reaction with a symmetry criterion. The indexes n and m are the number of carbon atoms of the species involved in this reaction according to equation 1.

$$k_{ps(n,m)} = k_{0ps} \times \exp\left(-\left(\frac{a_{ps}}{n} + b_{ps} \times \left(m - \frac{n}{2}\right)^2\right)\right) \quad (20)$$

$$\text{with } 3 \leq n \leq 20; m \leq n - 2$$

Chain Growth: the rate constant was calculated using equation 21 adapted from Pinto [14], where  $k_{0cg}$  accounts for the intensity of the chain growth reaction;  $a_{cg}$  and  $b_{cg}$  relate to the rate of reaction with the reacting olefins. The indexes n and m are the number of carbon atoms of the species involved in this reaction according to equation 2.

$$k_{cg(n,m)} = k_{0cg} \times \exp\left(-\left(a_{ps} \times n + \frac{b_{ps}}{m}\right)\right) \quad (21)$$

$$\text{with } 2 \leq n \leq 20; 2 \leq m \leq 20$$

Hydride Transfer: The rate constant was calculated using equation 22 adapted from Pinto [14], where  $k_{0ht}$  accounts for the

intensity of the hydride transfer reaction;  $a_{ht}$  and  $b_{ht}$  relates to the rate of reaction with the reacting olefins and paraffins, respectively. The indexes n and m are the number of carbon atoms of the species involved in this reaction according to equation 3.

$$k_{ht(n,m)} = k_{0ht} \times \exp\left(-\left(a_{ht} \times n + \frac{b_{ht}}{m}\right)\right) \quad (22)$$

$$\text{with } 2 \leq n \leq 20; 2 \leq m \leq 20$$

$\beta$ -Scission: The rate constant was calculated using equation 23 adapted from Pinto [14], where  $k_{0bs}$  accounts for the intensity of the  $\beta$ -scission reaction;  $a_{bs}$  relates the rate of reaction with the reacting olefin and  $b_{bs}$  relates the rate of reaction with one of the formed olefins. The indexes n and m are the number of carbon atoms of the species involved in this reaction according to equation 4.

$$k_{bs(n,m)} = k_{0bs} \times \exp\left(-\left(\frac{a_{bs}}{n} + \frac{b_{bs}}{m}\right)\right) \quad (23)$$

$$\text{with } 5 \leq n \leq 20; 2 \leq m \leq 18$$

Aromatic Formation: the rate constant was calculated using equation 24. Unlike the previous equations used to calculate constant rates of reaction, this equation is not from Pinto [14]. It has a pre-exponential factor,  $k_{0ar(m)}$ , related to intensity of the aromatic formation reaction and since were only considered aromatics between 6 and 8 carbon atoms there is a different value of  $k_{0ar}$  for each value of m, which did not happen in the previous reactions. It also has a parameter in the exponential,  $a_{ar}$ , which relates to the reacting olefins that will form paraffins, which is similar to  $a_{ht}$  from the

hydride transfer reaction. The indexes n and m are the number of carbon atoms of the species involved in this reaction according to equation 5.

$$k_{ar(n,m)} = k_{0ar(m)} \times \exp(-a_{ar} \times n) \quad (24)$$

with  $2 \leq n \leq 20$ ;  $6 \leq m \leq 8$

Isomerization forward reaction: the rate constant, was calculated using an exponential function (equation 25), with a pre-exponential factor,  $k_{0iso}$ , related to the intensity of the forward reaction; and a parameter in exponential,  $a_{iso}$ , related with the reacting linear paraffin. The index n are the number of carbon atoms of the species involved in this reaction according to equation 6.

$$k_{iso(n)} = k_{0iso} \times \exp(-a_{iso} \times n) \quad (25)$$

with  $4 \leq m \leq 20$

Isomerization equilibrium constant: it was determined by an empirical correlation between the sum of the isomerization equilibrium constants for a certain number of carbon atoms and the number of carbon atoms, n.

$$K_{(n)} = 0.0284e^{0.901n} \quad (26)$$

## Implementation of the model

In order to implement this model, it was used Euler method through a sub-routine in VBA which follows the following set of steps:

- 1) Calculate  $r_{(i,j)}$  using one the equations 10-14.
- 2) Calculate  $F_t^o$  using:

$$F_t^o = F_t^e + \sum_{i=1}^{21} \sum_{j=1}^4 r_{(i,j)} \times V \quad (21)$$

- 3) Calculate  $F_{(i,j)}^o$  using:

$$F_{(i,j)}^o = F_t^o \times \frac{P_{(i,j)}}{P_t} \quad (22)$$

- 4) Calculate  $\frac{\Delta N_{(i,j)}}{\Delta t}$  using:

$$\frac{\Delta N_{(i,j)}}{\Delta t} = F_{(i,j)}^o - F_{(i,j)}^e + r_{(i,j)} \quad (23)$$

- 5) Calculate The new  $N_{(i,j)}$  using:

$$N_{(i,j)}(t + \Delta t) = N_{(i,j)}(t) + \frac{\Delta N_{(i,j)}}{\Delta t}(t) \times \Delta t \quad (24)$$

- 6) Calculate The new  $P_{(i,j)}$  using:

$$P_{(i,j)} = \frac{N_{(i,j)}}{\sum_{i=1}^{21} \sum_{j=1}^4 N_{(i,j)} + N_{inert}} \times P_t \quad (25)$$

## Results and Discussion

The model was fitted to the experimental data obtain by Borges [15]. It was fitted for the catalytic cracking of n-heptane with a partial pressure in the feed of 0.42 atm over an H-ZSM5 catalyst and then tested for n-hexane and n-octane with partial pressures in the feed of 0.48 atm and 0.23, atm, respectively.

### n-Heptane

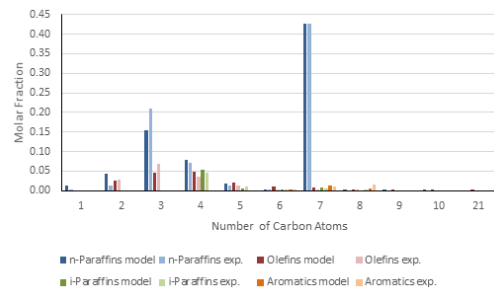


Figure 3 - Reactor outlet stream molar compositions for catalytic cracking of n-heptane

comparing model and experimental results using a partial pressure of reactant in the feed of 0.42 atm.

In order to fit the model results to experimental data, the parameters value set was varied to match the same level of conversion.

The conversion obtained with the model (57.32%) is very close to experimental conversion (57.47%).

The model can produce a good qualitative prediction of the product distribution. However, the model presents significant discrepancies for C<sub>2</sub> and C<sub>3</sub>. This fact is of great importance because propane is one of the main products of the catalytic cracking of heptane. The main problem is the fact that the asymmetry observed in the protolytic scission between the C<sub>3</sub> and C<sub>4</sub> should be higher. However, after several simulations with different value sets for the parameters involved in the protolytic scission and hydride transfer, the asymmetry between C<sub>3</sub>-C<sub>4</sub> did not suffer significant changes. The lacking of propane is offset by excess of methane and ethane mainly from secondary cracking. This fact must be related with the equation used to calculate the rate constants for the protolytic scission reaction.

The model can make an average prediction for branched paraffins and a good one for aromatics. The exception is aromatics with 8 carbon atoms because the amount and octenes predicted by the model is insufficient to produce the observed amounts and xylenes and ethyl-benzene.

Although all of these small discrepancies between the model and the experimental results, it still make a good O/P ratio prediction. The O/P ratio predicted by

the model is 0.46 while the experimental is 0.41. The model's output average molecular weight was also very close to the one obtained experimentally. The model predicted an output average molecular weight of 73.81 while the one obtained experimentally was 71.85.

## n-Hexane

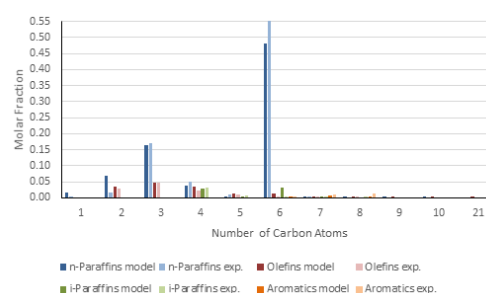


Figure 4 - Reactor outlet stream molar compositions for catalytic cracking of n-hexane comparing model and experimental results using a partial pressure of reactant in the feed of 0.48 atm.

The conversion obtained with the model (51.80%) are close to experimental conversion (44.63%) but with errors that cannot be overlooked. Although the model cannot accurately predict the conversion for n-hexane, it still can make a good prediction of the product distribution as can also be observed by output average molecular weight. The value predicted by the model was 67.67 while the one obtained experimentally was 70.01. However, it has a few exceptions, such as: methane, ethane and branched hexanes.

The O/P ratio values are also close. The model predicted a value of 67.67 while the one obtained experimentally was 70.01. This difference can be explained by excess of these paraffins mentioned before.

Unlike when the reactant is n-heptane, when the reactant is n-hexane the model



can make an accurate prediction for the molar fraction of propane which is the major product and this accuracy increases and the partial pressure of reactant in the feed increases. However this accuracy results of the symmetry of the primary cracking self-imposed by the model and not because it really can predict the molar fraction of propane since propane has 3 carbon atoms and hexane has 6 carbon atoms.

## n-Octane

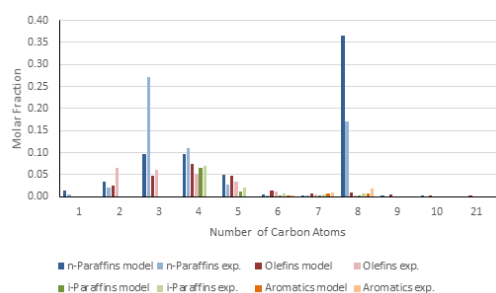


Figure 5 - Reactor outlet stream molar compositions for catalytic cracking of n-octane comparing model and experimental results using a partial pressure of reactant in the feed of 0.23 atm.

The model completely fails to predict the conversion since the model conversion (63.47%) presents huge discrepancies when compared to experimental conversion (82.95%). This fact leads to large errors in the prediction of the product distribution as be observed in Figure 5. The major problem, as observed for n-heptane as reactant, is the fact that it cannot accurately predict the molar fraction of propane.

The output average molecular weight predicted by the model (78.78) is always considerably higher than the experimental (62.95). As the conversion is much lower in the model, the output average molecular weight will have a greater contribution of the reactant which is heavier than most of the

major products. This will also have a huge impact in the O/P ratio too.

The O/P ratio value predicted by the model (0.63) is considerably higher than the obtained experimentally (0.41). As the reactant is not accounted in the calculation of the O/P ratio, the fact that the conversion is much lower in the model increases the model's O/P ratio value since the main differences between the model results and experimental results are the molar fractions of propane and n-octane.

## Conclusions

The study developed in this work consisted in analyzing a semi-empirical model to describe the complex kinetic network involved in catalytic cracking, The model is based on an pathways approach where the kinetic rate constants for elementary steps are obtain from empirical equations that relate the kinetic rate constant with the size and nature of the reactants and products. This work shows that these types of model present a significant potential to be used for the description of these complex networks as they can be described with some detail using a limited number of kinetic parameters. The use of a mathematical description for the kinetic parameters for a family of reactions using an empirical parameterized rationale allows us to tune the reaction so as to fit the model to existing data.

Through this work it can be concluded that the protolytic scission was the reaction that had the most impact regarding the distribution of the major products, C<sub>2</sub>-C<sub>4</sub>.

Reactions, such as:  $\beta$ -scission, chain growth and hydride transfer are also

important reactions, in particular regarding the O/P ratio.

The model presented in this work showed for feeds with reactants with more than 7 carbon atoms, the model still needs further optimization.

The equation used to calculate the protolytic scission rate constants need some adjustments in order to enable the model to make better predictions of the molar fraction of propane, which is the major product for the catalytic cracking of small paraffins. The deviations in this lump increase considerably with the number of carbon atoms of a pure reactant in the feed, as the model was not able to capture the asymmetry of the product distribution in relation to the point corresponding to half the size of the original hydrocarbon

Before the implementation of this model to real FCC feedstocks, more lumps and more reactions must be introduced first for a better understanding of this complex reaction network.

The experimental results used to develop this model has H-ZSM5 as catalyst. This zeolite has a low tendency to promote coke formation which was observed in this work. However, the fact that the model can be tuned to calculate the formation of coke, the addition of a parameter which accounts for the deactivation by coke would be of great use when applying this model to real FCC feedstocks.

## References

[1] F. C. Whitmore, *Ind. Eng. Chem.*, vol. 26, no. 1, pp. 94–95, 1934.  
[2] B. A. Williams, S. M. Babitz, J. T. Miller, R. Q. Snurr, and H. H. Kung, *Appl. Catal. A Gen.*, vol. 177, no. 2, pp. 161–175,

1999.  
[3] A. Kogelbauer and J. A. Lercher, *J. Catal.*, vol. 125, no. 1, pp. 197–206, 1990.  
[4] J. Abbot, *Appl. Catal.*, vol. 47, no. 1, pp. 33–44, 1989.  
[5] W. F. Pansing, *J. Phys. Chem.*, vol. 69, no. 2, pp. 392–399, 1965.  
[6] B. S. Greensfelder, H. H. Voge, and G. M. Good, *Ind. Eng. Chem.*, vol. 41, no. 11, pp. 2573–2584, 1949.  
[7] W. O. Haag and R. M. Dessau, *Proceedings of the 8th International Congress on Catalysis*, 1984, vol. 2, p. 305.  
[8] S. Kotrel, H. Knözinger, and B. C. Gates, *Microporous Mesoporous Mater.*, vol. 35–36, pp. 11–20, 2000.  
[9] A. Corma and A. V. Orchillés, *Microporous Mesoporous Mater.*, vol. 35–36, pp. 21–30, 2000.  
[10] L. Riekerti and J. Q. Zhou, *J. Catal.*, vol. 137, no. 2, pp. 437–452, 1992.  
[11] D. B. Lukyanov, V. I. Shtral, and S. N. Khadzhiev, *J. Catal.*, vol. 146, no. 1, pp. 87–92, 1994.  
[12] G. Giannetto, S. Sansare, and M. Guisnet, *J. Chem. Soc., Chem. Commun.*, no. 16, pp. 1302–1303, 1986.  
[13] A. Kumar and M. T. Klein, *ACS Div. Fuel Chem. Prepr.*, vol. 44, no. 3, pp. 485–489, 1999.  
[14] R. R. Pinto, “Kinetic Modelling of Catalytic Cracking Reactions,” Instituto Superior Técnico, 2004.  
[15] P. Borges, “Acidity-Activity Correlations for the Transformation of Hydrocarbons Over ZSM-5 Zeolites,” Instituto Superior Técnico, 2005.